ACS OMEGA

http://pubs.acs.org/journal/acsodf

Article

Hydrolysis Mechanism of Water-Soluble Ammonium Polyphosphate Affected by Zinc Ions

Zhengjuan Yan, Yan Wang, Dehua Xu,* Jingxu Yang, Xinlong Wang, Tao Luo, and Zhiye Zhang

Cite This: *ACS Omega* 2023, 8, 17573−17582

Read Online

ACCESS | Metrics & More | Article Recommendations | Supporting Information

ABSTRACT: Ammonium polyphosphate (APP) as a chelated and controlled-release fertilizer has been widely used in agriculture, and its hydrolysis process is of significance for its storage and application. In this study, the hydrolysis regularity of APP affected by Zn^{2+} was explored systematically. The hydrolysis rate of APP with different polymerization degrees was calculated in detail, and the hydrolysis route of APP deduced from the proposed hydrolysis model was combined with the conformation analysis of APP to reveal the mechanism of APP hydrolysis. The results show that Zn^{2+} decreased the stability of the P−O−P bond by causing a conformational change in the polyphosphate due to chelation, which in turn promoted APP hydrolysis. Meanwhile, Zn^{2+} caused the hydrolysis of polyphosphates with a high polymerization degree in APP to be switched from a terminal chain scission to an intermediate chain scission or various coexisting routes, affecting orthophosphate release. This work provides a theoretical basis and guiding significance for the production, storage, and application of APP.

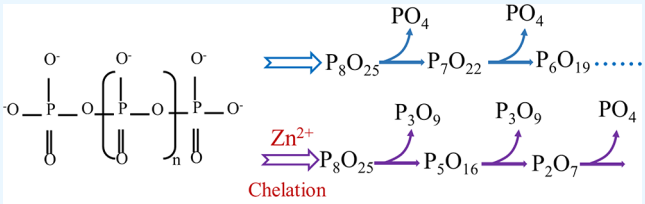

Ammonium polyphosphate hydrolysis

1. INTRODUCTION

Ammonium polyphosphate (APP, $(NH_4)_{n+2}P_nO_{3n+1}$) has been widely used as an inorganic polymer. High-polymerization-degree APP (average degree of polymerization, $n > 20$) is insoluble in water and has outstanding thermal stability, which makes such APPs suitable for flame retardant and fireproof applications.[1−3] Low-polymerization-degree APP ($n < 20$) has superior water solubility and is an important raw material in water-soluble, chelated, and controlled-release fertilizers.[4−7] The phosphorus in APP fertilizers exists as more than one species, including orthophosphates and polyphosphates (poly-Ps), the latter having different chain lengths. The poly-P in APP can chelate Fe, Al, Mg, Zn, Ca, Mn, etc., preventing or reducing P fixation during fertilizer configuration and soil application.[8] Poly-P can be hydrolyzed under suitable conditions. Meanwhile, the crop predominantly absorbs P in the form of orthophosphate (P_1).[9,10] Understanding the characteristics and mechanism of APP hydrolysis is of great significance for its production, storage, and application.

The hydrolysis of APP is affected by various factors such as its own chain length and concentration, temperature, pH, enzymes, and metal ions.[11−14] Generally, with higher temperature and lower pH, the hydrolysis rate of APP is accordingly increased.[15−17] The hydrolysis of APP is 10^6 times slower in the absence of an enzyme.[18,19] The action of metal ions on poly-P hydrolysis is quite complicated. Variable effects (i.e., deceleration/inhibition, acceleration, or no impact) of metal ions on poly-P hydrolysis are observed, and three mechanisms have been mentioned in previous studies:[20−24] (1) changing the poly-P conformation; (2) catalysis; (3) influencing the activity of the H^+ ions, or forming a complex with poly-P and thus competing with H^+ ions. Steveninck et al.[24] reported that Ni^{2+} increased the stability of the P−O−P bond by causing a conformational change in poly-P to inhibit its hydrolysis ($n > 2$) but had no significant impact on the conformation and hydrolysis of pyrophosphate (P_2). Frazier and Dillard[25] demonstrated that Fe and Al can promote the hydrolysis of poly-Ps ($n > 2$) but retard the hydrolysis of P_2. However, the response of hydrolysis of different APPs with different coexisting P species to metal ions and the changes in poly-P species during hydrolysis are not well understood. Besides, the hydrolysis of poly-P ($n > 3$) can occur via diverse pathways, including the breakage of the phosphoanhydride (P−O−P) bonds at the terminal and middle groups.[26] Huang et al.[26] and Wan et al.[27] reported that a terminal-only pathway via one-by-one cleavage of the terminal phosphate is the dominant hydrolysis pathway. However, how the metal ions affect the chain scission mode is unknown.

Zinc is one of the necessary nutrients for crop growth.[28−30] To our knowledge, there have been no studies focusing on the effect of Zn^{2+} on APP hydrolysis. This study aims to explore the kinetics and mechanism of APP hydrolysis affected by

Received: November 29, 2022
Accepted: April 28, 2023
Published: May 11, 2023

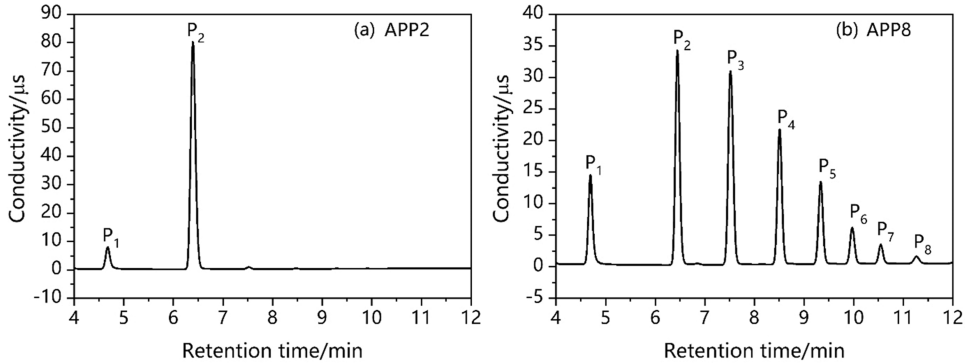

Figure 1. Chromatograms for water-soluble APPs used in this experiment measured by ion chromatography. (P_1, orthophosphate; P_2, pyrophosphate; P_3, tripolyphosphate; P_{3m}, trimetaphosphate; P_4, tetrapolyphosphate; P_5, pentapolyphosphate; P_6, hexapolyphosphate; P_7, heptapolyphosphate; and P_8, octapolyphosphate).

Zn^{2+}. Specifically, the changes in P speciation with time and the hydrolysis rate of APP with different P species (i.e., polymerization degree) distribution were determined. The hydrolysis route of APP deduced from the proposed hydrolysis model was combined with the conformation analysis of APP to reveal the mechanism of APP hydrolysis affected by Zn^{2+}.

2. MATERIALS AND METHODS

2.1. Materials. The raw materials used in this experimental study were water-soluble APP with weight-average polymerization degrees of 1.92 (APP2, model 18-58-0) and 3.14 (APP8, model 11-37-0). APP2 was produced by a kneading machine at a molar ratio of monoammonium phosphate (MAP) to urea of 1:0.5. MAP and urea are both analytically pure (provided by Chengdu Cologne Chemical Co. Ltd.). APP8 was provided by the Sino-Linchem Group. The P species distribution of the two APPs is shown in Figure 1 and Table S1. Analytically pure $ZnSO_4{\cdot}7H_2O$ was supplied by Chengdu Cologne Chemical Co. Ltd. The water used in the experiment is ultrapure water (resistivity ≥ 18 MΩ·cm) from a laboratory system.

2.2. Treatments. A series of APP2 solutions containing 0, 1.0, 2.0, 3.0, 4.0, 5.0, 6.0, and 8.0% Zn^{2+} and APP8 solutions containing 0, 0.5, 1.0, 2.0, 4.0, 6.0, and 8.0% Zn^{2+} were prepared. For each solution, APP2 (0.5 g) or APP8 (1.0 g) was dissolved and diluted with water, and then a certain concentration of $ZnSO_4{\cdot}7H_2O$ was added. Then, the solutions were transferred to the volumetric flasks, and the volumes were made up to 250 mL. One flask was left without the addition of Zn^{2+} as a blank control.

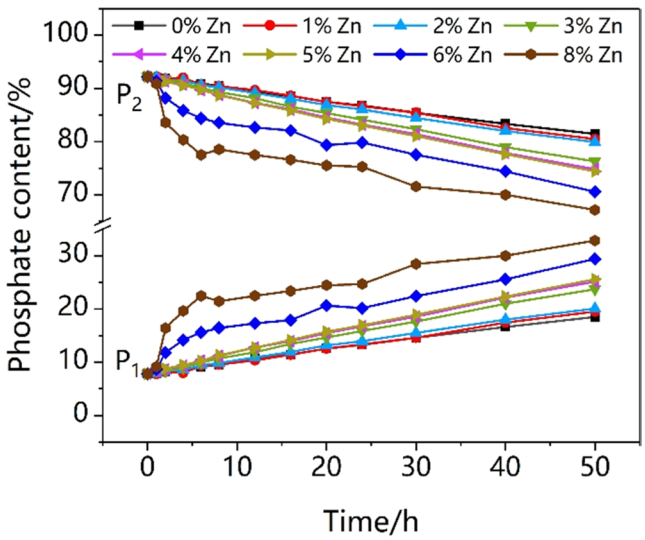

Figure 2. Effect of different concentrations of Zn^{2+} on the hydrolysis of APP2 (P_1, orthophosphate; P_2, pyrophosphate).

$$C_1 = \frac{m_1}{m_2 + m_3} \tag{1}$$

where C_1 represents the concentration of Zn^{2+}, and m_1, m_2, and m_3 represent the masses of Zn^{2+}, $ZnSO_4{\cdot}7H_2O$, and P_2O_5, respectively.

The solutions were transferred from the volumetric flasks to separate beakers, and 0.5 M HNO_3 was added to each beaker until a pH of 6 was reached. Then, the beakers were covered with lids, and the solutions were heated to 60 °C. The APP2 and APP8 solutions were sampled and analyzed at different time points to obtain the distribution of polyphosphate polymers. The APP2 solutions were monitored at 0, 1, 2, 4, 6, 8, 12, 16, 20, 24, 30, 40, and 50 h, and the APP8 solutions were monitored at 0, 1, 2, 4, 8, 12, 16, 20, 26, 32, 40, 50, 60, and 80 h.

2.3. Characterizations. *2.3.1. Ion Chromatography Analysis.* In this experiment, the P species in the APP solutions were monitored in real time using the ion chromatography method of Xie et al.[31] A Thermo Scientific ICS-600 chromatography system with an AS50 automated sampler and an ED50 electrochemical detector was used for the P speciation analysis.[32] Samples were injected into the ion-exchange column at intervals. KOH was used as an eluent with a gradient increase in concentration from an initial value of 30 mM to a terminal value of 80 mM. The flow rate of the KOH eluent was controlled at 1.2 mL·min^{-1}. The analytical column temperature was adjusted to 30 °C. Approximately 1.3 μL of the sample was injected, and the gradient elution time was 20 min.[31,33]

2.3.2. Reaction Infrared Spectroscopy. The functional groups of APP solutions with different Zn concentrations were studied in the initial phase of the reaction by an in situ reaction infrared (ReactIR) spectrometer (ReactIR 15, Mettler Toledo, Switzerland) with a wavenumber range of 650−3000 cm^{-1} and a resolution of 4 cm^{-1}. The infrared spectra of pure water and the sample solution were measured, respectively, and the spectra of APP solutions with Zn^{2+} shown in this work were

https://doi.org/10.1021/acsomega.2c07642
ACS Omega 2023, 8, 17573−17582

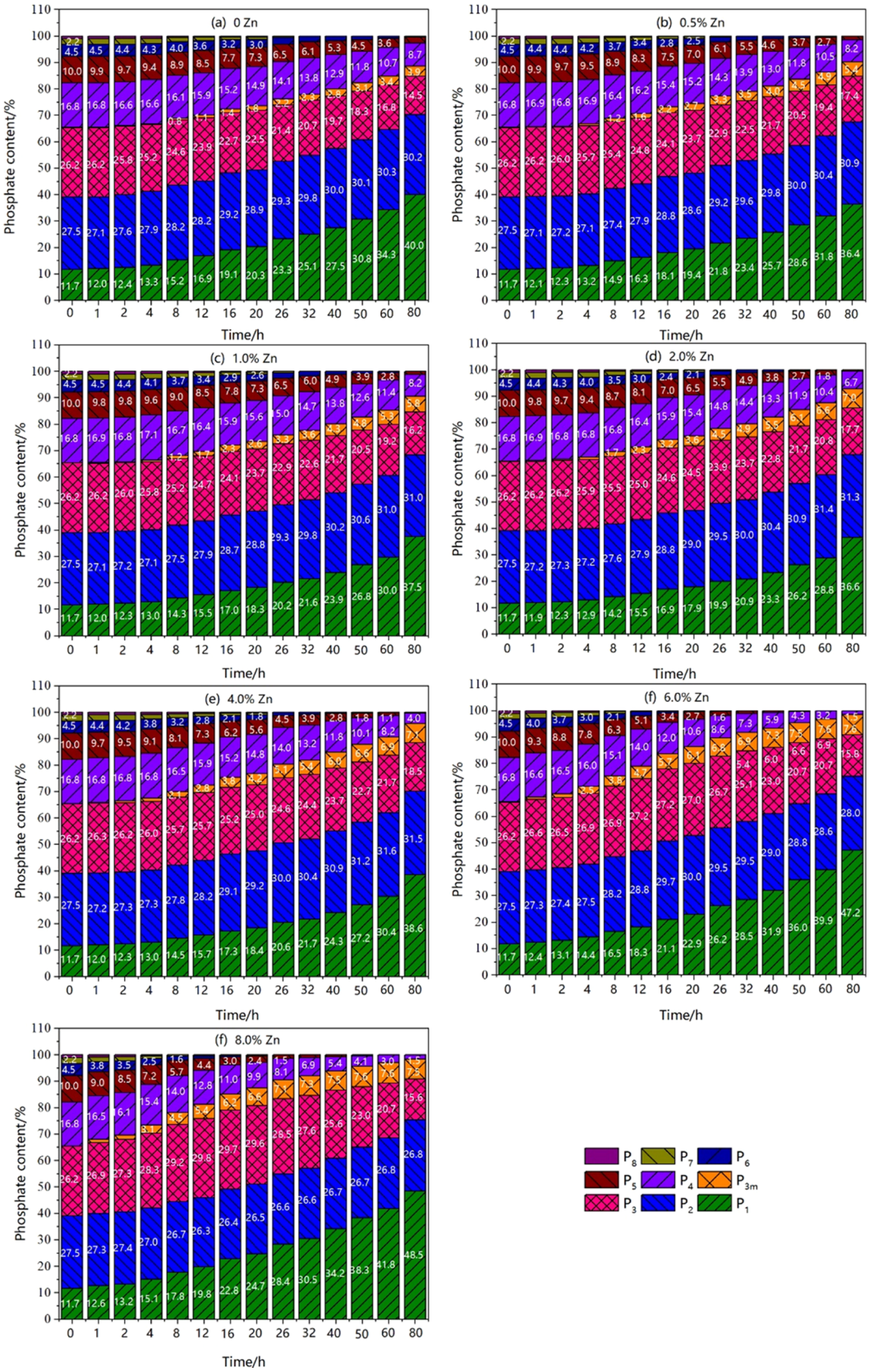

Figure 3. Effect of different concentrations of Zn^{2+} on the hydrolysis of APP8 (P_1, orthophosphate; P_2, pyrophosphate; P_3, tripolyphosphate; P_{3m}, trimetaphosphate; P_4, tetrapolyphosphate; P_5, pentapolyphosphate; P_6, hexapolyphosphate; P_7, heptapolyphosphate; and P_8, octapolyphosphate).

obtained by subtracting the spectra of pure water as the background.

2.3.3. Reaction Raman Spectroscopy. The chemical structures of the species in the sample solution with the

https://doi.org/10.1021/acsomega.2c07642
ACS Omega 2023, 8, 17573−17582

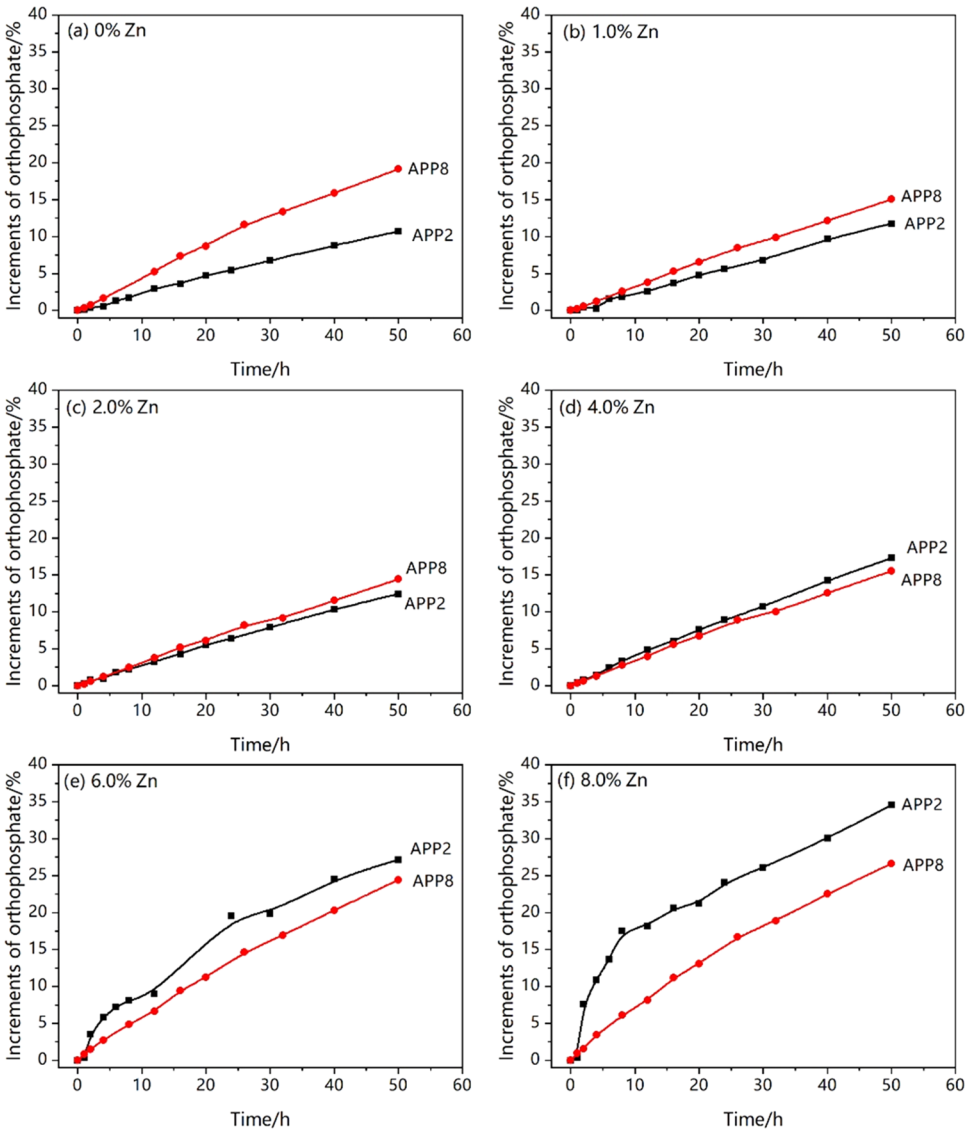

Figure 4. Changes in orthophosphate content over time in the two APP solutions at the same Zn^{2+} concentration.

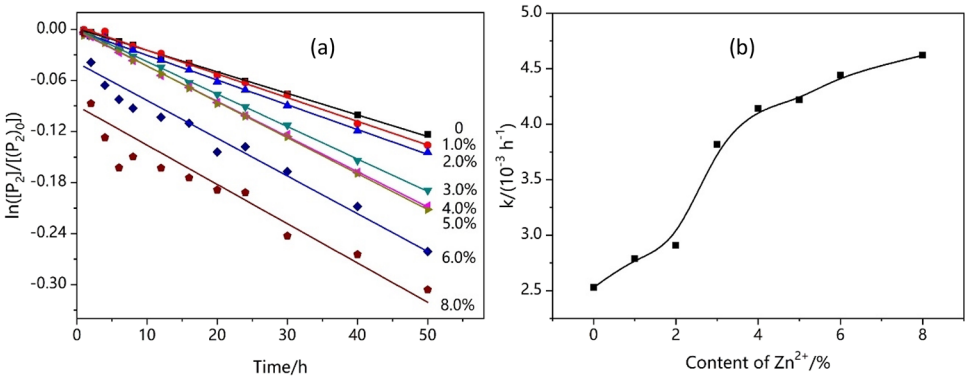

Figure 5. Fitting curve of the hydrolysis rate constant (k) of APP2 based on the first-order model (a) and k-value changes with increasing Zn^{2+} concentration (b) (P_2 and $(P_2)_0$ represent the percentage of P_2 content in the total P in APP2 at the reaction time and initial stage, respectively.).

highest Zn concentrations were analyzed with a Reaction Raman (React Raman) spectrometer (React Raman 785, Mettler Toledo). The Raman spectra were collected in the wavenumber range of 100−3000 cm^{-1} with an excitation wavelength of 785 nm.

3. RESULTS AND DISCUSSION

3.1. Changes in P Speciation with Time. Zn^{2+} concentrations in APP solutions affected the hydrolysis of poly-Ps in APPs (Figures 2 and 3). Figure 2 shows that the content of P_2 in the APP2 solution continuously decreased

https://doi.org/10.1021/acsomega.2c07642
ACS Omega 2023, 8, 17573−17582

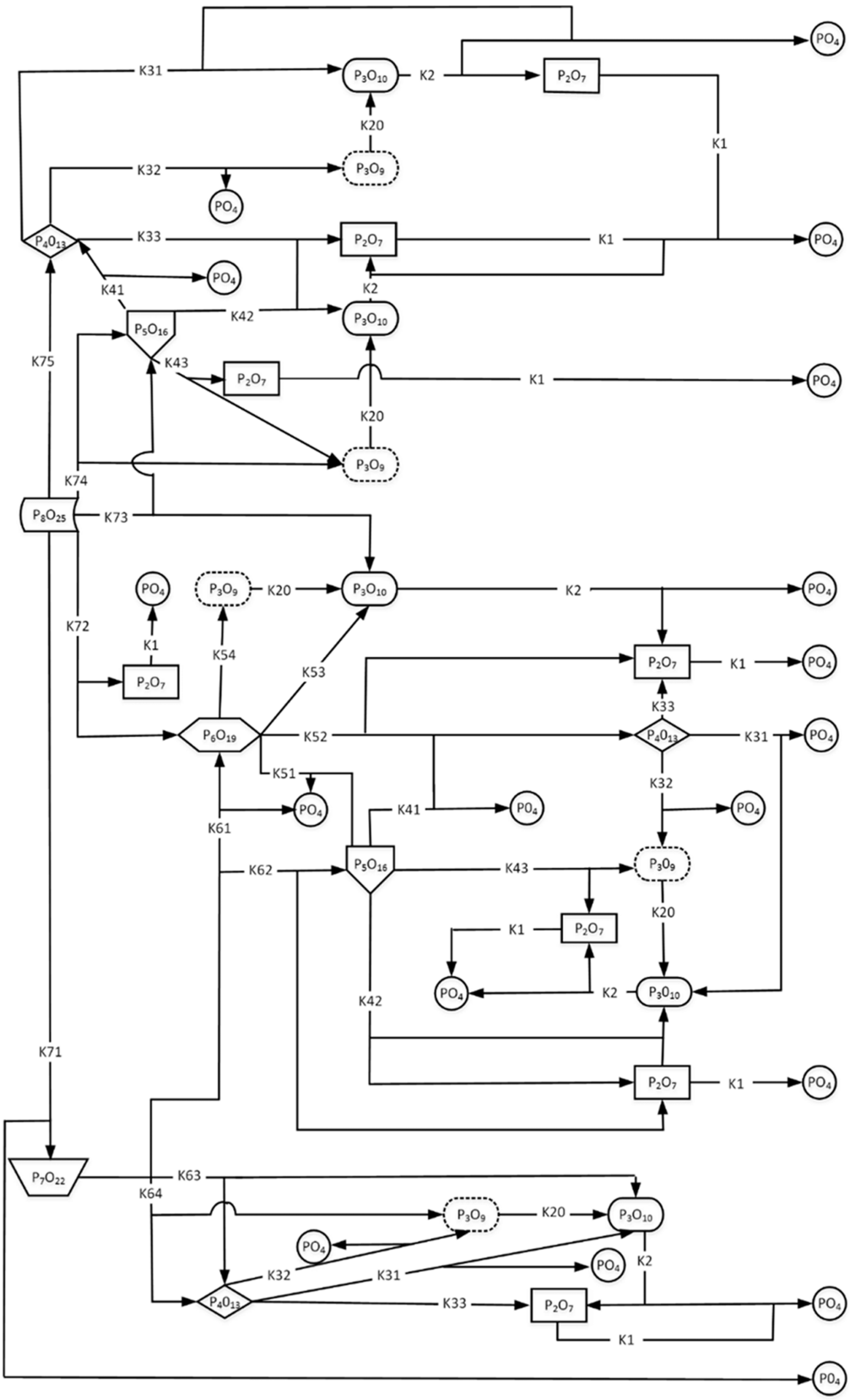

Figure 6. Hydrolysis reaction model of APP8.

while the content of P_1 increased. The content of P_2 decreased faster in the APP2 solution with a higher Zn^{2+} concentration, and the values after 50 h were 81.5, 80.5, 79.9, 76.3, 74.9, 74.4, 70.6, and 67.2% in the APP_2 solution with Zn^{2+} concentrations of 0, 1, 2, 3, 4, 5, 6, and 8%, respectively. In addition, when the Zn^{2+} concentration was in the ranges of 0−2, 3−5, and 6−8%, the rate of hydrolysis of the sample solution in each

https://doi.org/10.1021/acsomega.2c07642
ACS Omega 2023, 8, 17573−17582

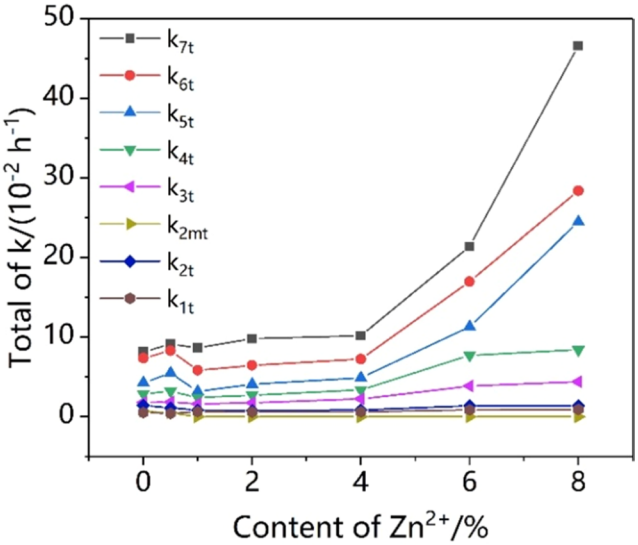

Figure 7. Effect of Zn^{2+} concentration on the total reaction rate of a group of phosphate species starting from one polymerization degree.

concentration interval did not change much, but the rate of hydrolysis increased significantly from one interval to the next.

Figure 3 shows that, in each APP8 solution, the contents of tetrapolyphosphate (P_4), pentapolyphosphate (P_5), hexapolyphosphate (P_6), heptapolyphosphate (P_7), and octapolyphosphate (P_8) decreased, while the content of P_1 and trimetaphosphate (P_{3m}) increased over time. The P_3 content decreased continuously in the solutions with Zn^{2+} concentrations ≤4%, but it but first increased and then decreased in the solution with 6 or 8% Zn^{2+}. The P_2 content increased slowly in the solution with Zn^{2+} concentrations ≤4%, but it first increased and then decreased in the solution with 6% of Zn^{2+} and reduced continuously in the solution with 8% Zn^{2+}. In addition, the decrease of poly-Ps with $n > 3$ in APP8 was higher in the solution with a higher Zn^{2+} concentration. However, compared to pure APP8 solution, a lower P_1 content in the APP8 solutions with 0.5−4% Zn^{2+} and a higher P_1 content in APP8 solutions with 6−8% Zn^{2+} were observed. This suggests that Zn^{2+} favored the hydrolysis of poly-Ps with a higher polymerization degree (e.g., $n > 3$), but only a high Zn^{2+} concentration could promote P_1 release in the APP8 solution.

Further, the P_1 release of two APP solutions under the same Zn^{2+} concentration was compared (Figure 4). The increment of P_1 in the APP8 solution was larger than that in the APP2 solution under the condition of Zn^{2+} concentration <4%, while the former was lower than the latter under the condition of Zn^{2+} concentration ≥4%. Previous studies reported that the hydrolysis of water-soluble APP with a high polymerization degree is faster than that of dimers,[34] and end-group cleavage is the dominant pathway for the hydrolysis of poly-Ps ($n > 3$).[26,27] In this study, APP8 contains poly-Ps ($n > 2$), which should contribute to the higher P_1 release compared to APP2 with P_2 only under the condition of low Zn^{2+} concentration. However, the promoting effect of Zn^{2+} on P_1 release by APP2 was stronger than that by APP8 under the condition of high Zn^{2+} concentration.

3.2. Hydrolysis Kinetics. *3.2.1. APP2.* The hydrolysis reaction model of P_2 is as follows:

$$P_2O_7 \rightarrow PO_4 + PO_4 \tag{2}$$

In this study, the hydrolysis of P_2 followed the first-order kinetic model (Figure 5a), which was consistent with the finding of Williard and Hatfield.[35] The rate equation is shown in eq S1 in the Supporting Information. The slope implies the reaction rate constant (k) in Figure 5a. As shown in Figure 5b, with the increase of Zn^{2+} concentration, the hydrolysis rate of the APP2 solution gradually increased, but the curve had a tendency to gradually level off, indicating that the hydrolysis rate of APP could hardly increase further if the Zn^{2+} concentration continued to increase. The changes in the APP conformation induced by Zn^{2+} due to chelation affected the hydrolysis rate of APP2. The change in the hydrolysis rate corresponded to a change in the APP conformation when Zn^{2+} was incorporated into the solution (Figures 8 and 9; the details are shown in Section 3.3.2). Thus, this implies that Zn^{2+} can chelate with APP, thereby facilitating hydrolysis. However, when APP becomes saturated with Zn, the hydrolysis rate of APP could not be altered by a further increase of Zn^{2+}.

3.2.2. APP8. The P species with the highest degree of polymerization in the sample solution APP8 is P_8, and five possible hydrolysis routes were considered. The specific hydrolysis model is shown in Figure 6. Considering the whole series of hydrolysis reactions involving 22 reaction rate constants (k_{71}, k_{72}, k_{73}, k_{74}, k_{75}, k_{61}, k_{62}, k_{63}, k_{64}, k_{51}, k_{52}, k_{53}, k_{54}, k_{41}, k_{42}, k_{43}, k_{31}, k_{32}, k_{33}, k_{20}, k_2, and k_1), the total hydrolysis rates of P_8, P_7, P_6, P_5, P_4, P_{3m}, P_3, and P_2 are expressed by eqs 3−10.

$$k_{71} + k_{72} + k_{73} + k_{74} + k_{75} = k_{7t} \tag{3}$$

$$k_{61} + k_{62} + k_{63} + k_{64} = k_{6t} \tag{4}$$

$$k_{51} + k_{52} + k_{53} + k_{54} = k_{5t} \tag{5}$$

$$k_{41} + k_{42} + k_{43} = k_{4t} \tag{6}$$

$$k_{31} + k_{32} + k_{33} = k_{3t} \tag{7}$$

$$k_{20} = k_{2mt} \tag{8}$$

$$k_2 = k_{2t} \tag{9}$$

$$k_1 = k_{1t} \tag{10}$$

P_8 follows a first-order reaction within the scope of this study. According to the hydrolysis reaction model, the rate equations can be obtained following eqs S2−S10. Using the least-squares fitting, the reaction rate constants with different Zn^{2+} concentrations were obtained, as shown in Table S2. The reaction rate constant was brought into the differential equation, and integration was used to obtain the distribution of the polymerization degree under different Zn^{2+} concentrations at different times after fitting; the obtained value was compared with the experimental value, as shown in Figure S1 and Table S3. From the verification results, the fitting was proven to be good, and the fitted values were basically consistent with the experimental ones.

The total reaction rate of each group of P species starting from one polymerization degree under this condition can be calculated as a function of Zn^{2+} concentration according to eqs 3−10, and the results are shown in Figure 7. It can be seen that poly-P with a higher polymerization degree showed faster hydrolysis. Moreover, Zn^{2+} increased the hydrolysis rate of poly-Ps ($n > 3$), especially under the higher Zn^{2+} concentration condition, but had a limited effect on the hydrolysis rates of P_3 and P_2. Frazier and Dillard[25] also demonstrated that Fe and Al

https://doi.org/10.1021/acsomega.2c07642
ACS Omega 2023, 8, 17573−17582

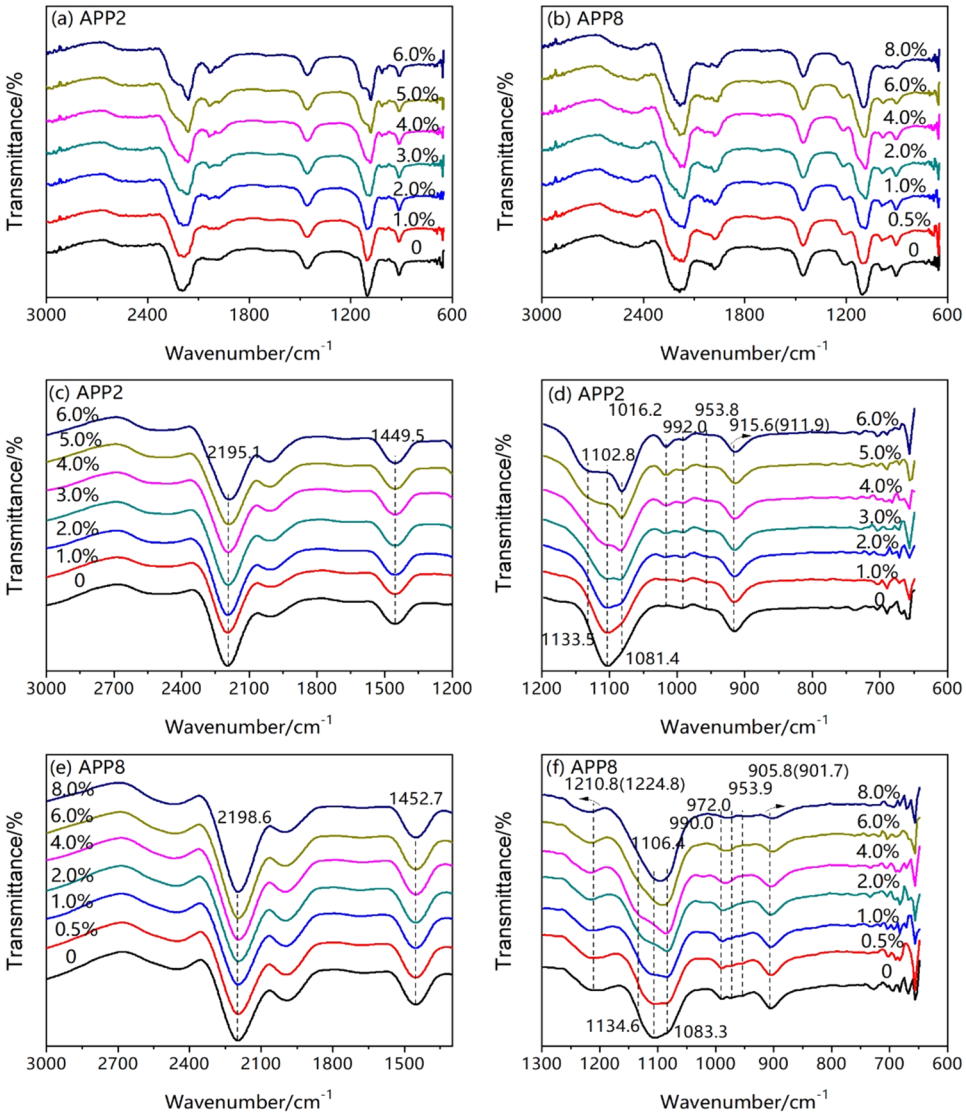

Figure 8. In situ infrared spectra of APP2 and APP8 solutions at different Zn^{2+} concentrations: (a, b) overall shape of the infrared spectra of APP2 and APP8 solutions; (c, d) partial shape of the infrared spectra of APP2 solutions; (e, f) partial shape of the infrared spectra of APP8 solutions.

can promote the hydrolysis of poly-Ps ($n > 2$) but retard the hydrolysis of P_2. However, Steveninck et al.[24] reported that Ni^{2+} inhibited the hydrolysis of poly-P ($n > 2$) but had no significant impact on the hydrolysis of P_2.

3.3. Hydrolysis Mechanism. *3.3.1. Hydrolysis Route.* The hydrolysis of poly-P ($n > 3$) can occur via diverse pathways, including the breakage of the phosphoanhydride (P−O−P) bonds at the terminal and middle groups.[26] When a hydrolysis pathway has a very small hydrolysis rate constant compared to other hydrolysis pathways, this indicates that the hydrolysis chain scission of APP basically does not follow this pathway. Therefore, we analyzed the hydrolysis route of each poly-P in the APP8 solution at different Zn^{2+} concentrations according to the hydrolysis rate constant of each route. Table S2 shows that the end-group cleavage is the only/dominant pathway for the hydrolysis of poly-Ps ($n > 3$), which was consistent with the results of Huang et al.[26] and Wan et al.[27] However, Zn^{2+} caused the hydrolysis of poly-Ps to be switched from a terminal chain scission to an intermediate chain scission or various coexisting routes, which explained why the P_1 release of APP8 was lower than that of APP2 under the higher Zn^{2+} concentration condition (Figure 4). The change of the chain scission model diminishes the advantage of breaking the terminal P of poly-Ps ($n > 3$) in APP8. In contrast, APP2 has a higher dimer concentration and can only hydrolyze to P_1, which contributed to the higher P_1 release at high Zn^{2+} concentrations compared to APP8. Besides, at high Zn^{2+} concentrations, the hydrolysis of P_2 is more frequent, resulting in an increase in P_1 release (Figure 2).

3.3.2. Conformation of APP. Changes in the conformation of poly-P induced by metal ions are considered to be responsible for the changes in poly-P hydrolysis. Zn^{2+} and APP can chelate, which in turn could result in the change of the APP conformation. Thus, we further analyzed the APP conformation affected by Zn^{2+} based on infrared and Raman spectra.

Figure 8 shows the ReactIR spectra of APP2 and APP8 solutions containing different Zn^{2+} concentrations. The ReactIR spectra of $ZnSO_4$ and monoammonium phosphate solutions are shown in Figures S2 and S3, respectively. The overall shape of the ReactIR spectra of APP2 solutions containing Zn^{2+} was similar to that of the blank APP2 solution

https://doi.org/10.1021/acsomega.2c07642
ACS Omega 2023, 8, 17573−17582

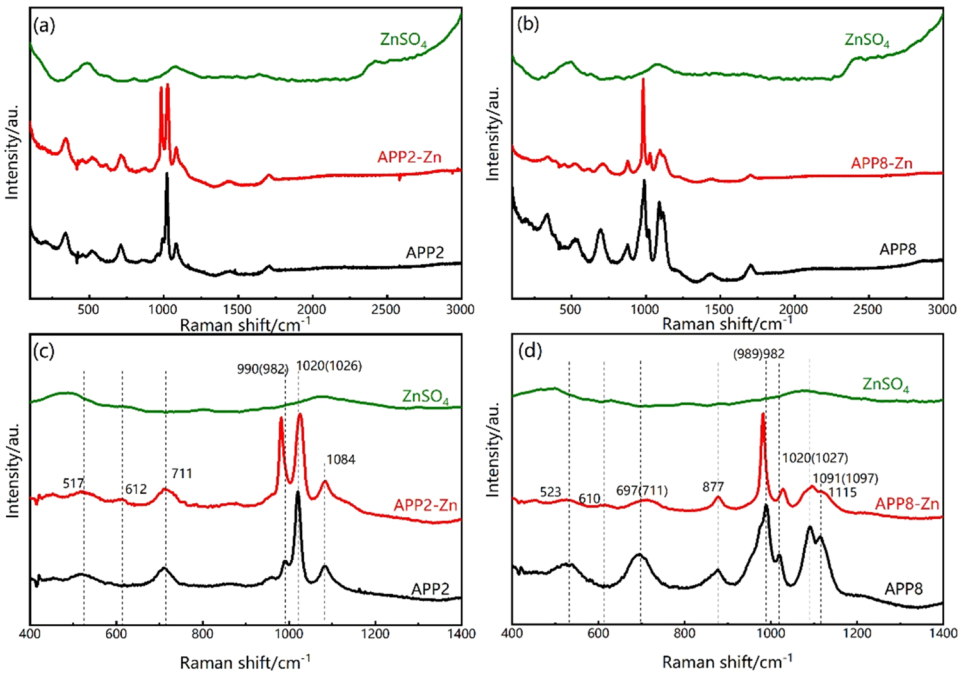

Figure 9. Raman spectra of APP2 and APP8: overall shapes of the Raman spectra of (a) APP2 and (b) APP8; (c) partial shapes of the Raman spectra of APP2 and (d) APP8.

(Figure 8a), indicating that the energies of PO_4 units within the polymers did not change and thus a change in the average shape of the chains was not expected to change upon addition of Zn. However, some infrared absorption peaks of APP2 with Zn^{2+} had changed obviously (Figure 8c,d). With the increase of Zn^{2+} concentration, the absorption peak of P−O−P at a wavenumber of 915.6 cm^{-1} was red-shifted, indicating that bond vibration was easier, and thus, it was expected to be more easily broken,[36] which can promote APP2 hydrolysis (Figures 2 and 5). The peak corresponding to O═P−O at a wavenumber of 1102.8 cm^{-1} had split into two new peaks at wavenumbers of 1081.4 and 1133.5 cm^{-1}, respectively. This indicated that the adjacent O═P−O in the APP molecular structure was connected to the same Zn^{2+}, formed a ring structure, and resulted in a vibration coupling phenomenon,[37] suggesting the occurrence of chelation between Zn^{2+} and APP. The peaks of N−H at a wavenumber of 1449.5 cm^{-1} and the peaks of P−H at 2195.1 cm^{-1} did not change significantly. The general features of the infrared spectra and corresponding changes of peaks with the addition of Zn^{2+} (Figure 8b,e,f) were similar to those of APP2.

Figure 9a,b shows that the overall shapes of Raman spectra of APP solutions before and after the introduction of Zn^{2+} were similar. The vibration band of the phosphate bond is between 400 and 1400 cm^{-1};[38] enlarged images of this portion are shown in Figure 9c,d. The Raman peaks in Figure 9c at 517, 711, 990, 1020, and 1084 cm^{-1} are attributed to the bending modes of the tetrahedra of P−O and the stretching vibrations of P−O−P, P−O, P−O, and P═O, sequentially.[39] After the introduction of Zn^{2+}, a blue and red shift occurred at the Raman peak of 1020 and 990 cm^{-1}, respectively, and the peak intensity at 990 cm^{-1} was enhanced due to the superposition of the SO_4^{2-} and P−O stretching vibration peaks.[40] Meanwhile, the Raman peak attributed to the Zn−O respiratory vibration appeared at 612 cm^{-1}, thereby suggesting that the oxygen atom in APP forms a coordination bond with Zn^{2+}. This further confirmed the existence of a chelation reaction between Zn^{2+} and APP, which led to the conformation change of APP.[38] Figure 9d shows the partial Raman spectra of APP8, and the general conclusions that can be drawn were similar to those of APP2.

4. CONCLUSIONS

The effect of metal ions on the hydrolysis of APP is crucial for the production and application of APP. This study investigated the hydrolysis kinetics and mechanism of two APPs with different polymerization degree distributions affected by Zn^{2+}. It revealed that the effect of Zn^{2+} on the hydrolysis of APP depended on both the polymerization degree of poly-P and the concentration of Zn^{2+}. Zn^{2+} decreased the stability of the P−O−P bond by causing a conformational change in poly-P due to chelation, which in turn promoted APP2 (a dimer) hydrolysis and the release of P_1. However, Zn^{2+} obviously favored the hydrolysis of poly-Ps with a higher polymerization degree (e.g., $n > 3$) but had a limited effect on the hydrolysis of P_3 and P_2 in APP8. Meanwhile, Zn^{2+} caused the hydrolysis of poly-Ps to be switched from a terminal chain scission to an intermediate chain scission or various coexisting routes, which affected P_1 release from APP8. Consequently, P_1 release in the APP8 solution was higher than that in APP2 solution under the condition of no or lower Zn^{2+} concentrations, while the former was lower than the latter under the condition of higher Zn^{2+} concentrations. Thus, the polymerization degree of APP and the Zn^{2+} concentration should be considered overall to prevent APP hydrolysis during fertilizer configuration and transportation and to optimize P supply with a suitable hydrolysis rate for crops.

■ ASSOCIATED CONTENT

Supporting Information

The Supporting Information is available free of charge at https://pubs.acs.org/doi/10.1021/acsomega.2c07642.

https://doi.org/10.1021/acsomega.2c07642
ACS Omega 2023, 8, 17573−17582

Phosphorus species distribution in the water-soluble APPs used in this experiment; hydrolysis rate constants of water-soluble APP8 with different concentrations of Zn^{2+}; mean squared error of different phosphate contents in APP8; comparison of the experimental and fitted values of polyphosphate contents (a−g); in situ infrared spectra of $ZnSO_4$ solutions with concentrations corresponding to APP2-Zn and APP8-Zn solutions; in situ infrared spectra of MAP solutions; hydrolysis rate equations S1−S10 (PDF)

■ AUTHOR INFORMATION

Corresponding Author

Dehua Xu − *Ministry of Education Research Center for Comprehensive Utilization and Clean Processing Engineering of Phosphorus Resources, School of Chemical Engineering, Sichuan University, Chengdu 610065, China;* orcid.org/0000-0001-5385-9968; Email: dhxu@scu.edu.cn

Authors

Zhengjuan Yan − *Ministry of Education Research Center for Comprehensive Utilization and Clean Processing Engineering of Phosphorus Resources, School of Chemical Engineering, Sichuan University, Chengdu 610065, China;* orcid.org/0000-0002-8583-8173

Yan Wang − *Ministry of Education Research Center for Comprehensive Utilization and Clean Processing Engineering of Phosphorus Resources, School of Chemical Engineering, Sichuan University, Chengdu 610065, China*

Jingxu Yang − *Ministry of Education Research Center for Comprehensive Utilization and Clean Processing Engineering of Phosphorus Resources, School of Chemical Engineering, Sichuan University, Chengdu 610065, China*

Xinlong Wang − *Ministry of Education Research Center for Comprehensive Utilization and Clean Processing Engineering of Phosphorus Resources, School of Chemical Engineering, Sichuan University, Chengdu 610065, China;* orcid.org/0000-0002-5279-5859

Tao Luo − *Ministry of Education Research Center for Comprehensive Utilization and Clean Processing Engineering of Phosphorus Resources, School of Chemical Engineering, Sichuan University, Chengdu 610065, China;* orcid.org/0000-0002-7979-8048

Zhiye Zhang − *Ministry of Education Research Center for Comprehensive Utilization and Clean Processing Engineering of Phosphorus Resources, School of Chemical Engineering, Sichuan University, Chengdu 610065, China*

Complete contact information is available at: https://pubs.acs.org/10.1021/acsomega.2c07642

Notes

The authors declare no competing financial interest.

■ ACKNOWLEDGMENTS

The authors are grateful for financial support from the Natural Science Foundation of China (Project No. 32172677) and the Fundamental Research Funds for the Central Universities (China).

■ REFERENCES

(1) Zhao, C. X.; Liu, Y.; Wang, D. Y.; Wang, D. L.; Wang, Y. Z. Synergistic effect of ammonium polyphosphate and layered double hydroxide on flame retardant properties of poly (vinyl alcohol). *Polym. Degrad. Stab.* **2008**, *93*, 1323−1331.

(2) Annakutty, K. S.; Kishore, K. Flame retardant polyphosphate esters: 1. Condensation polymers of bisphenols with aryl phosphorodichloridates: synthesis, characterization and thermal studies. *Polymer* **1988**, *29*, 756−761.

(3) Braun, U.; Schartel, B.; Fichera, M. A.; Jäger, C. Flame retardancy mechanisms of aluminium phosphinate in combination with melamine polyphosphate and zinc borate in glass-fibre reinforced polyamide 6, 6. *Polym. Degrad. Stab.* **2007**, *92*, 1528−1545.

(4) El-Sayed, S. Ammonium polyphosphate and ammonium orthophosphate as sources of phosphorus for Jerusalem artichoke. *Alexandria Sci. Exch. J.* **2015**, *36*, 47−57.

(5) Dick, R. P.; Tabatabai, M. A. Polyphosphates as sources of phosphorus for plants. *Fert. Res.* **1987**, *12*, 107−118.

(6) Thilo, E.; Wieker, W. Study of degradation of polyphosphates in aqueous solution. *J. Polym. Sci.* **1961**, *53*, 55−59.

(7) Hughes, J. D.; Hashimoto, I. Triammonium Pyrophosphate as a Source of Phosphorus for Plants 1. *Soil Sci. Soc. Am. J.* **1971**, *35*, 643−647.

(8) Dick, R. P.; Tabatabai, M. A. Factors affecting hydrolysis of polyphosphates in soils. *Soil Sci.* **1987**, *143*, 97−104.

(9) Sipponen, M. H.; Rojas, O. J.; Pihlajaniemi, V.; Lintinen, K.; Österberg, M. Calcium chelation of lignin from pulping spent liquor for water-resistant slow-release urea fertilizer systems. *ACS Sustainable Chem. Eng.* **2017**, *5*, 1054−1061.

(10) Wang, L.; Deng, L.; Tu, P.; Yang, Y.; Gong, L.; Zhang, C. Research progress on hydrolysis factors of ammonium polyphosphate and its application in fertilizer. *Phosphate Compd. Fert.* **2015**, *30*, 25−27.

(11) Ahmad, F.; Kelso, W. I. Pyrophosphate as a source of phosphorus: Hydrolysis under different conditions. *J. Res. (Sci.)* **2001**, *12*, 130−139.

(12) McBeath, T. M.; Lombi, E.; McLaughlin, M. J.; Bünemann, E. K. Polyphosphate-fertilizer solution stability with time, temperature, and pH. *J. Plant Nutr. Soil Sci.* **2007**, *170*, 387−391.

(13) Lin, Y. P.; Singer, P. C. Inhibition of calcite crystal growth by polyphosphates. *Water Res.* **2005**, *39*, 4835−4843.

(14) Nannipieri, P.; Giagnoni, L.; Landi, L.; Renella, G. Role of Phosphatase Enzymes in Soil. In *Phosphorus in Action*; Springer, 2011; pp 215−243.

(15) Williard, J. W.; Farr, T. D.; Hatfield, J. D. Hydrolysis of ammonium pyro-, tripoly-, and tetrapolyphosphate at 25. deg. and 50. deg. *J. Chem. Eng. Data* **1975**, *20*, 276−283.

(16) Gilliam, J. W.; Sample, E. C. Hydrolysis of pyrophosphate in soils: pH and biological effects. *Soil Sci.* **1968**, *106*, 352−357.

(17) Wang, L.; Gong, L.; Deng, L.; Tu, P.; Yang, Y.; Guan, L.; Cheng, F.; Zhang, C. Effect of different temperature and pH on the hydrolysis of ammonium polyphosphate. *Phosphate Compd. Fert.* **2015**, *30*, 8−11.

(18) Ali Tabatabai, M. A.; Dick, W. A.Enzymes in Soil: Research and Developments in Measuring Activities. In *Enzymes in the Environment: Activity, Ecology, and Applications*; Marcel Dekker, Inc., 2002; pp 567−596.

(19) Reue, K.; Brindley, D. N. Thematic Review Series: Glycerolipids. Multiple roles for lipins/phosphatidate phosphatase enzymes in lipid metabolism. *J. Lipid Res.* **2008**, *49*, 2493−2503.

(20) Corbridge, D. E. C. Crystallographic data on some Kurrol salts. *Acta Crystallogr.* **1955**, *8*, 520.

(21) Jost, K. H. Zur Struktur des KURROLschen Silbersalzes ($AgPO_3$) x. *Z. Anorg. Allg. Chem.Chemie* **1958**, *296*, 154−156.

(22) Van Wazer, J. R. *Phosphorus and its Compounds*; Wiley-Interscience: New York, 1958.

(23) Thilo, E. Die kondensierten Phosphate. *Naturwissenschaften* **1959**, *46*, 367−373.

(24) van Steveninck, J. The Influence of metal ions on the hydrolysis of polyphosphates. *Biochemistry* **1966**, *5*, 1998−2002.

(25) Frazier, A. W.; Dillard, E. F. Ionic effects on the hydrolysis of polyphosphates in liquid fertilizers. *J. Agric. Food Chem.* **1981**, *29*, 695−698.
(26) Huang, R. X.; Wan, B.; Hultz, M.; Diaz, J. M.; Tang, Y. Z. Phosphatase-mediated hydrolysis of linear polyphosphates. *Environ. Sci. Technol.* **2018**, *52*, 1183−1190.
(27) Wan, B.; Yang, P.; Jung, H.; Zhu, M.; Diaz, J. M.; Tang, Y. Iron oxides catalyze the hydrolysis of polyphosphate and precipitation of calcium phosphate minerals. *Geochim. Cosmochim. Acta* **2021**, *305*, 49−65.
(28) He, Z. L.; Yang, X. E.; Stoffella, P. J. Trace elements in agroecosystems and impacts on the environment. *J. Trace Elem. Med. Biol.* **2005**, *19*, 125−140.
(29) Mousavi, S. R. Zinc in crop production and interaction with phosphorus. *Aust. J. Basic Appl. Sci.* **2011**, *5*, 1503−1509.
(30) Zhang, H.; Frey, M.; Navizaga, C.; Lenzo, C.; Taborda, J.; Taifan, W.; Sadeghnejad, A.; Sviklas, A. M.; Baltrusaitis, J. Dairy wastewater for production of chelated biodegradable Zn micronutrient fertilizers. *ACS Sustainable Chem. Eng.* **2016**, *4*, 1722−1727.
(31) Xie, W.-J.; Wang, X.-L.; Li, Y.-S.; Xu, D.-H.; Zhong, Y.-J.; Yang, J.-X. Simultaneous determination of various phosphates in water-soluble ammonium polyphosphate. *Chromatographia* **2019**, *82*, 1687−1695.
(32) Halliwell, D. J.; McKelvie, I. D.; Hart, B. T.; Dunhill, R. H. Hydrolysis of triphosphate from detergents in a rural waste water system. *Water Res.* **2001**, *35*, 448−454.
(33) Yang, J.; Kong, X.; Xu, D.; Xie, W.; Wang, X. Evolution of the polydispersity of ammonium polyphosphate in a reactive extrusion process: Polycondensation mechanism and kinetics. *Chem. Eng. J.* **2019**, *359*, 1453−1462.
(34) Yang, J.; Xie, W.; Kong, X.; Xu, D.; Wang, X. Reactive extrusion of ammonium polyphosphate in a twin-screw extruder: polydispersity improvement. *Chem. Eng. Process.* **2018**, *133*, 58−65.
(35) Williard, J. W.; Williard, J. W.; Hatfield, J. D. Hydrolysis of ammonium pyro-, tripoly-, and tetrapolyphosphate at 25. deg. and 50. deg. *J. Chem. Eng. Data* **1975**, *20*, 276−283.
(36) Frost, R. L. An infrared and Raman spectroscopic study of natural zinc phosphates. *Spectrochim. Acta, Part A* **2004**, *60*, 1439−1445.
(37) Rashchi, F.; Finch, J. A. Polyphosphates: a review their chemistry and application with particular reference to mineral processing. *Miner. Eng.* **2000**, *13*, 1019−1035.
(38) Berkani, S.; Dassenoy, F.; Minfray, C.; Martin, J. M.; Cardon, H.; Montagnac, G.; Reynard, B. Structural changes in tribo-stressed zinc polyphosphates. *Tribol. Lett.* **2013**, *51*, 489−498.
(39) De Jager, H.-J.; Heyns, A. M. Study of the hydrolysis of sodium polyphosphate in water using Raman spectroscopy. *Appl. Spectrosc.* **1998**, *52*, 808−814.
(40) Nakamoto, K.Infrared and Raman Spectra of Inorganic and Coordination Compounds. In *Theory and Applications in Inorganic Chemistry*; John Wiley & Sons, 2008; pp 88−97.

https://doi.org/10.1021/acsomega.2c07642
ACS Omega 2023, 8, 17573−17582